

Microphase Separation in Nonequilibrium Biomembranes

Pierre Sens¹ and Matthew S. Turner²

¹Laboratoire Gulliver, UMR 7083 CNRS-ESPCI, 10 rue Vauquelin, 75231 Paris Cedex 05 - France

²Department of Physics and Complexity Centre, University of Warwick, Coventry CV4 7AL, United Kingdom

(Received 6 October 2010; published 6 June 2011)

Compositional heterogeneities of cell membranes are thought to play an important role in many physiological processes. We study how variations in the membrane composition can be driven by nonthermal fluctuating forces and therefore show how these can occur relatively far from any critical point for the membrane. We show that the membrane steady state is not only controlled by the strength of the forces and how they couple to the membrane, but also by their dynamics: In a simple class of models this is captured by a single force correlation time. We conclude that the coupling of membrane composition to normal mechanical forces, such as might be exerted by polymerizing cytoskeleton filaments, could play an important role in controlling the steady state of a cell membrane that exhibits transient lateral modulations of its composition on length scales in the 10–100 nm regime.

DOI: 10.1103/PhysRevLett.106.238101

PACS numbers: 87.16.dj, 87.16.dt, 87.16.Xa

Biological membranes are composed of a large variety of lipids and proteins. Spatiotemporal variations of membrane composition play an important role for many cellular functions, including cell signaling, endocytosis, and cellular trafficking [1,2], and are likely to be tightly regulated. The lateral organization of biomembranes has, in particular, been linked to the structure of the cell cytoskeleton [3–5]. It is becoming increasingly clear that the control of biomembrane organization involves the stochastic dynamics of its environment, which influences the membrane through biochemical signaling, mechanical perturbation, and direct material fluxes. Recently we showed how recycling of membrane components can sensitively tune the state of the membrane [6]. Here we show how membrane organization depends on the temporal correlations of its fluctuating environment. We first calculate the membrane's response to a locally correlated stochastic coupling of arbitrary origin. We then analyze in detail the case in which membrane composition is coupled to the local membrane curvature, itself driven by random mechanical forces generated by the cytoskeleton. This nonequilibrium regulatory mechanism makes it unnecessary to invoke critical fluctuations, and hence a fine-tuning of membrane composition, to explain membrane heterogeneity on the observed length scales.

Biological membranes can be studied *in vivo* via dynamical tracking of tagged membrane components [3]. Recently, small (~ 75 nm), short-lived (~ 250 msec) domains have been observed near well-defined membrane locations [7,8]. Such behavior appears to result from spatially localized stochastic forces of biochemical or physical origin that act to drive changes in membrane composition.

Model for membrane phase separation.—We start with the membrane Hamiltonian [9]:

$$\mathcal{H} = \frac{1}{2} \int d^2\mathbf{r} [b\phi^2 + \mu(\nabla\phi)^2 + \kappa(\nabla^2 u)^2 + \sigma(\nabla u)^2 - 2\kappa C'_o \phi \nabla^2 u - 2\zeta\phi - 2fu], \quad (1)$$

written in terms of the membrane composition field $\phi(\mathbf{r})$ and normal membrane displacement $u(\mathbf{r})$, both assumed to represent small perturbations around a perfectly mixed ($\phi = 0$) and flat ($u = 0$) membrane. Equation (1) can either be motivated on symmetry grounds or by tracing the physical interpretation of the various terms. These include local mixing interaction and concentration gradient terms for the membrane composition (parameters b and μ), the membrane tension σ and bending rigidity κ , and a coupling term C'_o capturing how the local membrane spontaneous curvature depends on the composition to lowest (linear) order in ϕ . Thus, when the latter term is considered, ϕ is the density of membrane component(s) that couple to curvature. The fields f and ζ are external (cellular) forces conjugate to u and ϕ , respectively. In Fourier space [with $x_{\mathbf{q}} = \int d^2\mathbf{r} e^{i\mathbf{q}\cdot\mathbf{r}} x(\mathbf{r})$ and $x_{-\mathbf{q}}^* = x_{\mathbf{q}}$], $\mathcal{H} = \int \frac{d^2\mathbf{q}}{2(2\pi)^2} \mathcal{H}_{\mathbf{q}}$ with

$$\begin{aligned} \mathcal{H}_{\mathbf{q}} &= h_{\mathbf{q}} |\phi_{\mathbf{q}}|^2 + k_{\mathbf{q}} |u_{\mathbf{q}}|^2 - 2\beta_{\mathbf{q}} u_{\mathbf{q}} \phi_{\mathbf{q}}^* - 2\zeta_{\mathbf{q}} \phi_{\mathbf{q}}^* - 2f_{\mathbf{q}} u_{\mathbf{q}}^*, \\ h_{\mathbf{q}} &= b + \mu q^2, \quad k_{\mathbf{q}} = \sigma q^2 + \kappa q^4, \quad \beta_{\mathbf{q}} = \kappa C'_o q^2. \end{aligned} \quad (2)$$

The kinetic evolution of the fields u and ϕ , coupled to the local fluctuating forces $f(t)$ and $\zeta(t)$, is given by [10]

$$\begin{aligned} \dot{\phi}_{\mathbf{q}} + \Lambda q^2 (h_{\mathbf{q}} \phi_{\mathbf{q}} - \beta_{\mathbf{q}} u_{\mathbf{q}}) &= \Lambda q^2 \zeta_{\mathbf{q}}, \\ \eta q \dot{u}_{\mathbf{q}} + (k_{\mathbf{q}} u_{\mathbf{q}} - \beta_{\mathbf{q}} \phi_{\mathbf{q}}) &= f_{\mathbf{q}}, \end{aligned} \quad (3)$$

where Λ is related to the diffusion coefficient of membrane components by $D = \Lambda h_{\mathbf{q}}$ [$D_o = D(q \rightarrow 0)$], and η is the solvent viscosity dampening membrane displacement [11]. The susceptibilities of the membrane deformation $k_{\mathbf{q}}$ and composition $h_{\mathbf{q}}$ involve characteristic length scales. The former $\lambda \equiv \sqrt{\kappa/\sigma}$ (~ 100 nm for $\kappa = 20k_B T$ and $\sigma = 10^{-5}$ J/m²) is quite relevant to the present study, while the latter $\sqrt{\mu/b}$ is of molecular dimension far from

the critical point for membrane composition [10], and will be neglected ($\mu \simeq 0$) when discussing specific examples below. Note that the q -space functions coupling the different fields in Eqs. (2) and (3) can readily be generalized to include additional contributions to the elastic and dynamical responses of both deformation and composition.

We study the membrane's response to correlated fluctuating forces (of zero mean), to which end we adopt

$$\begin{aligned} \langle \zeta_q(t) \rangle &= 0, & \langle \zeta_q(t) \zeta_{-q}(t + \delta t) \rangle &= \bar{\zeta}_q^2 e^{-|\delta t|/\tau_\phi}, \\ \langle f_q(t) \rangle &= 0, & \langle f_q(t) f_{-q}(t + \delta t) \rangle &= \bar{f}_q^2 e^{-|\delta t|/\tau}. \end{aligned} \quad (4)$$

For multiple localized forces we can write $f(\mathbf{r}, t) = \sum_i f_i(t) \delta(\mathbf{r} - \mathbf{r}_i)$, with f_i the force due to the i th cytoskeletal anchor (located in \mathbf{r}_i), similarly for ζ representing localized arbitrary biochemical coupling(s). Thus, $f_q = \sum_i e^{iq \cdot \mathbf{r}_i} f_i(t)$ with $\langle f_i(t) \rangle = 0$ and $\langle f_i(t) f_j(t + \delta t) \rangle = \bar{f}^2 \delta_{ij} e^{-\delta t/\tau}$ (with \bar{f} a constant). In what follows we concentrate on a single force center situated at $\mathbf{r} = 0$ noting that the membrane response is linear and so membrane deformation caused by additional force center(s) would simply add independently. For a numerical solution of the microphase separation induced by multiple force centers, see supporting movies 1–4 [12], while the level of interactions between these force centers is shown in Fig. 1.

Fluctuations of membrane composition.—We first study the fluctuations of membrane composition subjected to a correlated fluctuating force $\zeta(t)$ of arbitrary origin, without coupling to the membrane shape ($\beta_q = 0$). The solution of Eq. (3) subjected to Eq. (4) is calculated in the supplementary information (SI) [12]:

$$\langle |\phi_q|^2 \rangle = \frac{\bar{\zeta}_q^2}{h_q^2} \frac{Dq^2 \tau_\phi}{Dq^2 \tau_\phi + 1}. \quad (5)$$

This expression gives the appropriate static response ($\phi_q = \zeta_q/h_q$) in the limit $Dq^2 \tau \gg 1$, and satisfies equipartition of energy, $\langle |\phi_q|^2 \rangle = k_B T/h_q$, in the limit of temporally uncorrelated forces ($\tau_\phi \rightarrow 0$) if the fluctuating force $\zeta(t)$ satisfies the fluctuation-dissipation theorem, $\langle |\zeta_q|^2 \rangle = \bar{\zeta}_q^2 = k_B T/(\Lambda q^2 \tau_\phi)$. Equation (5) shows that modes satisfying $Dq^2 \tau_\phi \gg 1$ are essentially unaffected, while modes such that $Dq^2 \tau_\phi \ll 1$ are strongly suppressed, by the fluctuating nature of the correlated force.

Membrane-cytoskeleton coupling.—The cytoskeleton underlying the plasma membrane has long been thought to influence the mobility and clustering of membrane proteins by hindering their lateral motion [13]. The membrane composition is also known to be sensitive to the local membrane curvature [14], which should fluctuate strongly under the action of mechanical forces produced by (de)polymerizing cytoskeleton filaments, and molecular motors. Many membrane proteins and lipids possess a spontaneous curvature and tend to colocalize with membrane regions of particular curvature [15]. At the linear level, one may write the composition-dependent spontaneous

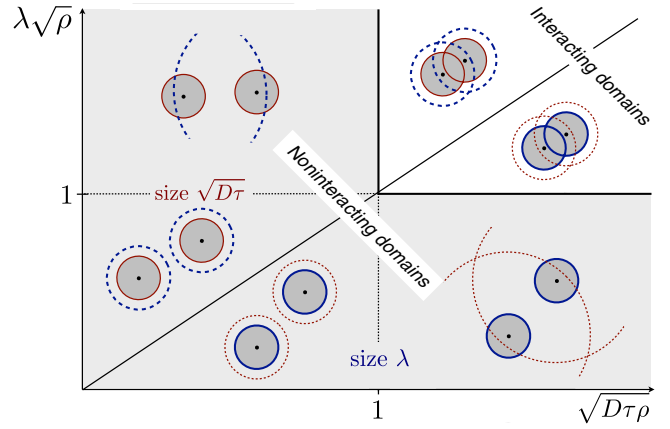


FIG. 1 (color online). The dynamics of a membrane containing multiple force centers (of density ρ) depends on the ratio of the membrane length λ (see text) to the distance between force centers, $\lambda\sqrt{\rho}$, and the ratio of the composition diffusion length $\sqrt{D\tau}$ to the distance between force centers $\sqrt{D\tau\rho}$. Each illustration represents two neighboring force centers, with a typical separation $\rho^{-1/2}$, and shows (not to scale) the diffusion length in red (thin), the membrane length in blue (thick), and the region of substantial compositional variation in dark gray shading. The controlling length scale is shown as a continuous colored line and the other length scale is shown dotted. The shaded region indicates where domains are substantially noninteracting.

curvature $C_0 = C'_0 \phi$, as was done in Eq. (1). One can in principle solve Eq. (3) for the two coupled fields of membrane composition and deformation [10]. For the sake of clarity here we only investigate the limit of rather weak coupling ($\beta_q \equiv \kappa C'_0 q^2 < \sqrt{k_q h_q}$), so that the membrane deformation is substantially determined by the external force, with little feedback from the membrane composition. In the opposite limit of strong coupling, a curvature instability can arise where large membrane undulations coupled to strong composition variation grow spontaneously [9]. Curvature-induced sorting of membrane components can also occur when the membrane rigidity κ depends on its composition [16,17]. This situation cannot be addressed at the linear level of description chosen here, but can be expected to yield qualitatively similar behavior.

The mean squared deformation solution of Eq. (3) under a fluctuating force f satisfying Eq. (4) is (see SI [12]) [18]:

$$\langle u_q(t) u_q(t + \delta t) \rangle = \frac{\bar{f}^2}{k_q^2 (\alpha_q \tau)^2 - 1} \left(e^{-\delta t/\tau} - \frac{e^{-\alpha_q \delta t}}{\alpha_q \tau} \right), \quad (6)$$

where $\alpha_q = k_q/(\eta q)$ is the relaxation rate of the membrane deformation [19]. As a result of its coupling to the local curvature, the membrane composition sees a fluctuating force following fluctuations of the membrane shape, with correlation $\langle \zeta'_q(t) \zeta'_q(t + \delta t) \rangle = \beta_q^2 \langle u_q(t) u_q(t + \delta t) \rangle$.

The composition correlation function now involves three relaxation rates: of the force correlation $1/\tau$, of the membrane deformation α_q , and of the membrane composition Dq^2 . In the regime of most interest to us the membrane

shape adjusts much faster than the membrane composition $\alpha_q \gg Dq^2$, since the membrane length λ ($= \sqrt{\kappa/\sigma} \sim 100$ nm) is much smaller than $\kappa/(D\eta)$ (~ 10 μ m). The membrane deformation can therefore be considered to relax instantaneously on the time scale of composition changes. The correlation functions then reads:

$$\langle |\phi_q|^2 \rangle = \frac{(\lambda^2 C'_0)^2 \bar{f}^2}{h_q^2 [1 + (\lambda q)^2]^2} \frac{Dq^2 \tau}{(Dq^2 \tau + 1)}, \quad (7)$$

akin to Eq. (5) but with an effective driving force that includes the membrane elasticity and the strength C'_0 of the composition coupling to curvature but which is insensitive to the deformation dynamics α_q .

Quantification of membrane organization.—We first examine the extent to which a static perturbation, to be specific a mechanical force \bar{f} generating membrane curvature, induces the reorganization of (curvature-sensitive) membrane components. The inverse Fourier transform of Eq. (7) in the limit $\tau \rightarrow \infty$ (and $\mu = 0$) reveals a spatial composition modulation around a static point force of the form $\phi_{|\tau \rightarrow \infty} = \phi_0 K_0(r/\lambda)$, with $\phi_0 = \bar{f} C'_0/b$. The modified Bessel function of the second kind K_0 , characteristics of membrane deformation [20], decays exponentially beyond a distance λ from the force [21] [see Fig. 2(b)]. Assuming the second virial coefficient b to be of thermal origin, $b \sim k_B T/s$, where s is a molecular area (e.g., the area of curvature-sensitive proteins), strong enrichment near the force ($\phi_0 \simeq 1$) is expected for $s > k_B T/\bar{f} C'_0$, of order $(2 \text{ nm})^2$ with $f = 5 \text{ pN}$ [18] and $1/C'_0 = 5 \text{ nm}$ [22]. Sorting of lipid alone [$s \sim (0.7 \text{ nm})^2$] typically requires proximity to a critical point ($b \rightarrow 0$) [16,22], but membrane proteins are often larger than the critical area and

their spatial distribution can be strongly sensitive to a membrane curvature generated by an external force [15].

The full spatiotemporal correlation function for the membrane composition (see SI [12]) can yield any statistical information of the membrane composition by inverse Fourier transform to real space [Fig. 2(b)]. This step typically involves numerical calculation, but an analytic statistical measure for the membrane state can be obtained by integrating the autocorrelation function:

$$\begin{aligned} C(\tau_\phi) &= \frac{\int d^2 \mathbf{r} \langle |\phi(\mathbf{r})|^2 \rangle_{|\tau_\phi} }{\int d^2 \mathbf{r} \langle |\phi(\mathbf{r})|^2 \rangle_{|\tau_\phi \rightarrow \infty} } \\ &= \frac{\int d^2 q (\bar{\xi}^2/h_q^2) [D\tau_\phi q^2 / (D\tau_\phi q^2 + 1)]}{\int d^2 q \bar{\xi}^2/h_q^2}, \quad (8) \end{aligned}$$

here normalized by the membrane's response to a permanent perturbation discussed above [$C(\tau_\phi \rightarrow \infty) = 1$] to reveal the role of the fluctuating nature of the force.

Equation (8) can readily be used to quantify the membrane composition's response to fluctuations of the local curvature under stochastic mechanical forces [using Eq. (7)]:

$$C_{\text{curv}} = \frac{\bar{\tau}(\bar{\tau} - \log \bar{\tau} - 1)}{(\bar{\tau} - 1)^2}, \quad (9)$$

with $\bar{\tau} \equiv D\tau/\lambda^2$. This result can be compared to the response of other types of fluctuating environments, such as an exponentially decreasing local source of signaling molecules $\bar{\xi}_q = 1/[1 + (\lambda q)^2]^{3/2}$, $C_{\text{exp}} = \bar{\tau}(\bar{\tau}^2 - 2\bar{\tau} \log \bar{\tau} - 1)/(\bar{\tau} - 1)^3$, or a similar force of Gaussian form, $\bar{\xi}_q = e^{-(\lambda q)^2/2}$. These response functions are shown in Fig. 2(a). All three show a slow convergence toward the static response ($C \rightarrow 1$ for $\bar{\tau} \rightarrow \infty$), but exhibit distinct behaviors for weakly correlated excitations:

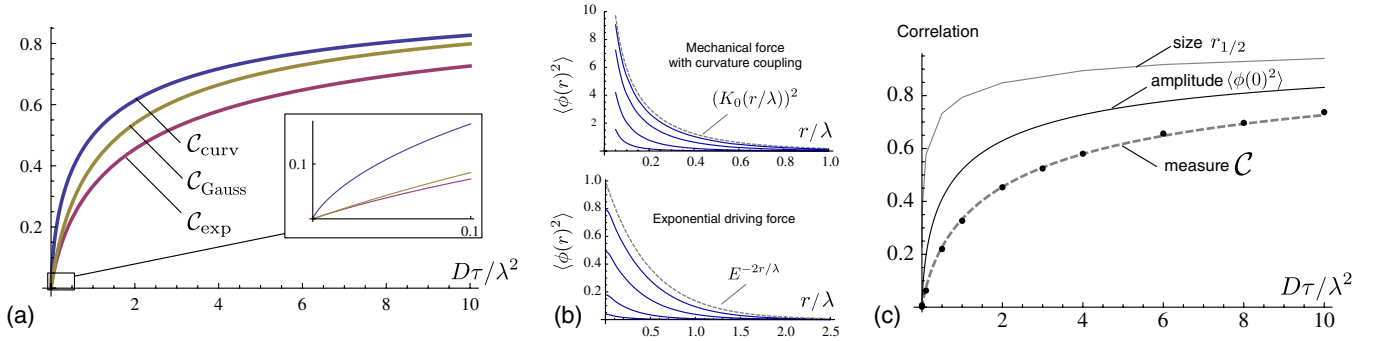


FIG. 2 (color online). (a) Comparison of the membrane dynamical response [as defined by Eq. (8)] to a fluctuating environment of typical correlation time τ that drives the membrane composition changes via (i) localized exponentially decreasing forces (C_{exp}), (ii) localized forces with Gaussian spatial distribution (C_{Gauss}), and (iii) a local coupling between membrane composition and membrane curvature, itself excited by localized normal mechanical forces (C_{curv}). The inset shows the different behaviors of the response functions for weak correlations: $\tau \rightarrow 0$. (b) Local correlation function $\langle \phi(r)^2 \rangle$ driven by a fluctuating random force at $r = 0$ with a correlation time τ (shown for $D\tau = 0.01, 0.1, 1, 10$). Top shows the case of a local mechanical driving force with coupling between membrane composition and curvature, bottom shows the case of a force decaying exponentially from a local source. The results for permanent forces ($\tau \rightarrow \infty$) are shown dashed. (c) Amplitude at the origin ($\langle \phi(0)^2 \rangle$ —black curve) and distance from the origin where the amplitude has dropped by half ($r_{1/2}$ —gray curve) as a function of the correlation time τ , shown for an exponential perturbation, which is well behaved as $r \rightarrow 0$ [21]. The global measure C (dashed gray curve) is numerically shown to follow the expected scaling behavior $C = \langle \phi(0)^2 \rangle r_{1/2}^2$ (dots).

$$C_{\text{curv}} \xrightarrow{\bar{\tau} \rightarrow 0} \bar{\tau} \log \frac{1}{\bar{\tau}}, \quad C_{\text{exp}} \sim C_{\text{Gauss}} \xrightarrow{\bar{\tau} \rightarrow 0} \bar{\tau}. \quad (10)$$

The membrane's deformation around a localized mechanical force contains a high density of short wavelength modes to which its composition adjusts quickly. C_{curv} is thus highly sensitive to short-time correlations of the stochastic environment. Note that Eqs. (9) and (10), are valid provided $\tau > a^2/D$, a weak constraint since the short-distance cutoff a is of molecular size.

Two important measures of the fluctuating membrane domains are the intensity of phase segregation within them and their average size. Both properties depend on the correlation time τ , and are somehow mixed in the global measure \mathcal{C} of Eq. (8). As shown in Fig. 2(b), the real-space correlation function $\langle \phi(r, t)^2 \rangle$ can be obtained from the (numerical) inverse Fourier transform of $\langle \phi_q(t) \phi_{q'}(t) \rangle$ (see SI [12]). These plots show that while the characteristic shape of the domain resembles the permanent shape even for short correlation time τ (of order $\sim \lambda^2/D$), its composition requires longer times to reach its static level. This behavior is further illustrated in Fig. 2(c), where both the maximal level of correlation ($\langle |\phi(a)|^2 \rangle$) and the typical distance $r_{1/2}$ from the source at which the mean squared amplitude falls by half ($\langle |\phi(r_{1/2})|^2 \rangle = \langle |\phi(a)|^2 \rangle / 2$) are plotted as a function of the correlation time. Remarkably, the global measure of the perturbation \mathcal{C} closely follows the expected scaling result $\mathcal{C} \sim \langle \phi(a)^2 \rangle r_{1/2}^2$ for all times, thereby validating \mathcal{C} as a good quantity with which to measure the membrane's response to a fluctuating environment.

Conclusion.—The processes that control the lateral organization of biological membranes are still elusive. Much effort has been put into understanding the equilibrium phase behavior of these membranes as part of a philosophy that sees them as quasiequilibrium structures. We believe that active fluctuations in the membrane's environment play a crucial role in controlling the membrane lateral heterogeneities. Our model shows the central importance of the temporal correlation of a noisy environment in triggering the membrane response; see Fig. 1.

Figure 2 shows how the membrane's lateral organization varies with the correlation time of the perturbation. While the spatial extent of the membrane reorganization approaches the extent of the driving force even in a highly fluctuating environment ($\bar{\tau} < 1$), the amplitude of the perturbation must be driven much more slowly ($\bar{\tau} \gg 1$) if it is to reach its full potential. For typical values of the parameters, $\lambda = 100$ nm and $D = 0.1 \mu\text{m}^2/\text{s}$, we find a typical diffusion time scale of order 100 msec, similar to the correlation time of membrane heterogeneities reported in [7]. This means that one can expect $\bar{\tau} \sim 1$ in this particular case, and that the present model can be very relevant to lateral heterogeneities of cellular membranes [7]. Dynamical maps of the cell membrane's composition [8] bear clear resemblance to the one produced by our model (in particular movie 4 in the SI [12]). A primary

result of this work is that compositional changes due to variations in membrane curvature driven by normal forces exerted by the cytoskeleton could represent the dominant cellular strategy for membrane organization. This proposal may be tested by monitoring the spatiotemporal dynamics of the membrane composition in conditions when the dynamics of cytoskeletal filaments has been modified, e.g., by specific drugs.

We thank the french ANR (P.S.) for financial support, and we thank the KITP (UCSB, Santa Barbara) where this work was initiated. M.S.T. acknowledges the support of EPSRC Grant No. EP/E501311/1.

-
- [1] K. Simons and E. Ikonen, *Nature (London)* **387**, 569 (1997).
 - [2] D.M. Engelman, *Nature (London)* **438**, 578 (2005).
 - [3] A. Kusumi and Y. Sako, *Curr. Opin. Cell Biol.* **8**, 566 (1996).
 - [4] G. Forgacs *et al.*, *J. Cell Sci.* **117**, 2769 (2004).
 - [5] M. Edidin, *Biophys. J.* **91**, 3963 (2006).
 - [6] M. S. Turner, P. Sens, and N. D. Socci, *Phys. Rev. Lett.* **95**, 168301 (2005).
 - [7] A. Sergé *et al.*, *Nat. Methods* **5**, 687 (2008).
 - [8] Dynamical maps of the cell membrane heterogeneities can be see at <http://www.nature.com/nmeth/journal/v5/n8/extref/nmeth.1233-S3.mov>, [7].
 - [9] S. Leibler, *J. Phys. (Paris)* **47**, 507 (1986).
 - [10] P. Chaikin and T. Lubensky, *Principles of Condensed Matter Physics* (Cambridge University Press, Cambridge, England, 1995).
 - [11] E. Reister-Gottfried, S.M. Leitenberger, and U. Seifert, *Phys. Rev. E* **81**, 031903 (2010).
 - [12] See supplemental material at <http://link.aps.org/supplemental/10.1103/PhysRevLett.106.238101> for detailed calculations and movies.
 - [13] A. Kusumi *et al.*, *Annu. Rev. Biophys. Biomol. Struct.* **34**, 351 (2005).
 - [14] R. Parthasarathy and J.T. Groves, *Soft Matter* **3**, 24 (2007).
 - [15] H.T. McMahon and J.L. Gallop, *Nature (London)* **438**, 590 (2005).
 - [16] B. Sorre *et al.*, *Proc. Natl. Acad. Sci. U.S.A.* **106**, 5622 (2009).
 - [17] M. Heinrich *et al.*, *Proc. Natl. Acad. Sci. U.S.A.* **107**, 7208 (2010).
 - [18] The small deformation approximation ($\nabla u < 1$) is valid provided $f < 2\pi\sqrt{2\kappa\sigma} \simeq 10$ pN, beyond which the membrane deforms into a tube. Cytoskeletal elements are known to be able to generate such large forces [15].
 - [19] Thermal equilibrium requires $\tau \rightarrow 0$ and $\bar{f}^2 = 2k_B T \eta q$.
 - [20] A.R. Evans, M.S. Turner, and P. Sens, *Phys. Rev. E* **67**, 041907 (2003).
 - [21] K_0 diverges logarithmically at short distance. Solutions must be regularized by introducing a short-length cutoff a , corresponding to the (molecular) lateral size over which the force acts (we assume $a \ll \lambda$).
 - [22] M.M. Kamal *et al.*, *Proc. Natl. Acad. Sci. U.S.A.* **106**, 22245 (2009).